Pediatric Radiology (2018) 48:1348–1363
https://doi.org/10.1007/s00247-018-4141-9

PEDIATRIC BODY MRI

Whole-body magnetic resonance imaging: techniques and non-oncologic indications

Mary-Louise C. Greer [1,2]

Received: 19 November 2017 / Revised: 11 February 2018 / Accepted: 16 April 2018

Abstract

Whole-body MRI is increasingly utilized for assessing oncologic and non-oncologic diseases in infants, children and adolescents. Focusing on the non-oncologic indications, this review covers technical elements required to perform whole-body MRI, the advantages and limitations of the technique, and protocol modifications tailored to specific indications. Rheumatologic diseases account for the majority of non-oncologic whole-body MRI performed in pediatric patients at the author's institution. Whole-body MRI helps in establishing the diagnosis, documenting disease extent and severity, and monitoring treatment response in enthesitis-related arthritis (ERA) and chronic recurrent multifocal osteomyelitis (CRMO). Other non-oncologic indications for whole-body MRI include osteomyelitis (usually pyogenic), pyrexia of unknown origin, neuromuscular disorders, inherited and inflammatory myopathies such as juvenile dermatomyositis and polymyositis, avascular necrosis, and fat/storage disorders. Use of whole-body MRI in postmortem imaging is rising, while whole-body MRI in non-accidental injury is considered to be of limited value. Imaging findings for a range of these indications are reviewed with whole-body MRI examples.

Keywords Children · Chronic recurrent multifocal osteomyelitis · Enthesitis-related arthritis · Myopathy · Osteomyelitis · Postmortem · Whole-body magnetic resonance imaging

Introduction

Whole-body MRI has evolved to evaluate an array of diseases in children, both oncologic and non-oncologic [1–5]. Whole-body MRI lends itself to pathologies that are diffuse, multifocal or affect different organ systems, providing excellent anatomical definition through high soft-tissue contrast and spatial resolution, and increasingly offering functional information [2, 4, 6, 7]. This is achieved without the risk of ionizing radiation common to other large field-of-view (FOV) imaging techniques such as CT and positron emission tomography (PET) [8–10]. Whole-body MRI is also typically performed without an intravenous gadolinium-based contrast agent (GBCA), with its own risk profile related to nephrogenic systemic fibrosis and tissue deposition [11–13]. These factors have propelled a steady expansion in the range of applications and overall utilization of whole-body MRI in the radiation-sensitive pediatric population.

At the author's institution, a tertiary pediatric hospital, the annual number of whole-body MRI examinations increased by 20% in 3 years, recently plateauing, related in part to institutional capacity (Fig. 1). Our whole-body MRI referrals for non-oncologic indications exceed those for oncologic indications by more than 2:1. Of these, approximately 80% are for two rheumatologic diseases: enthesitis-related arthritis (ERA), also known as juvenile spondyloarthritis, and chronic recurrent multifocal osteomyelitis (CRMO). Figure 2 shows the spectrum of our referrals over 12 months in 2017. By comparison, in an audit of pediatric whole-body MRI by Damasio et al. [14], most were for oncologic indications; however rheumatologic diseases were also the most common non-oncologic indications. Our referral pattern has changed slightly over time for a few reasons. Whole-body MRI is no longer part of *DICER1* syndrome surveillance at our institution since adoption of newly defined consensus guidelines [15–17]. Conversely, recently redefined recommendations for neuromuscular disorders have resulted in an increased demand for whole-body MRI [18, 19]. Postmortem whole-body MRI doubled from 13 in 2014 to 28 in 2017, in part from local factors,

✉ Mary-Louise C. Greer
mary–louise.greer@sickkids.ca

[1] Department of Diagnostic Imaging, The Hospital for Sick Children, 555 University Ave., Toronto, ON, M5G 1X8, Canada

[2] Department of Medical Imaging, University of Toronto, Toronto, ON, Canada

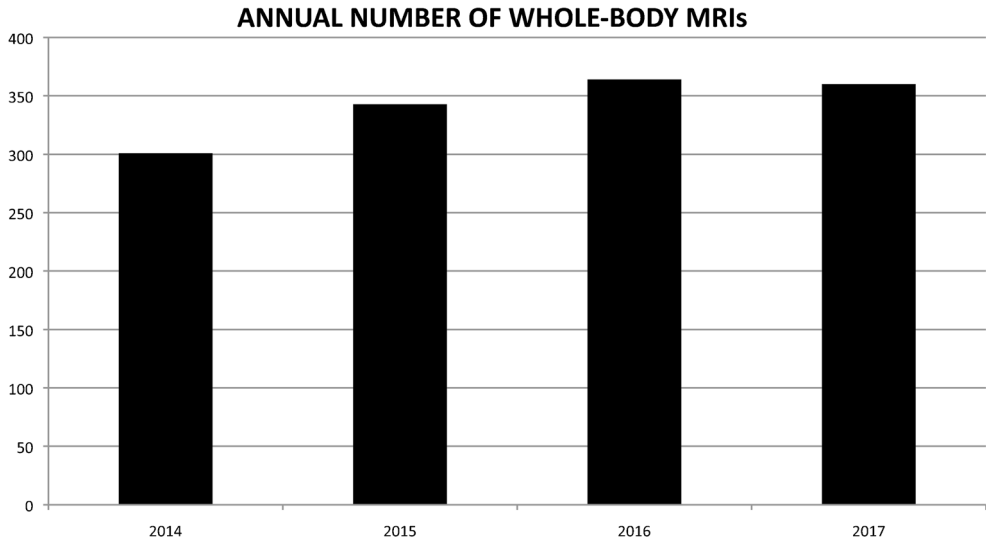

Fig. 1 Annual number of whole-body MRI studies at the author's institution

with greater access for forensic MRI and recent establishment of a postmortem imaging rotation for radiology residents. This upward trend is likely to continue because of the establishment of a European Society of Paediatric Radiology (ESPR) postmortem imaging task force in 2015 [20–22].

This review first centers on whole-body MRI technique, with an emphasis on non-oncologic indications. The author discusses technical elements to consider when performing whole-body MRI, advantages and limitations of the technique, and protocol modifications tailored for specific

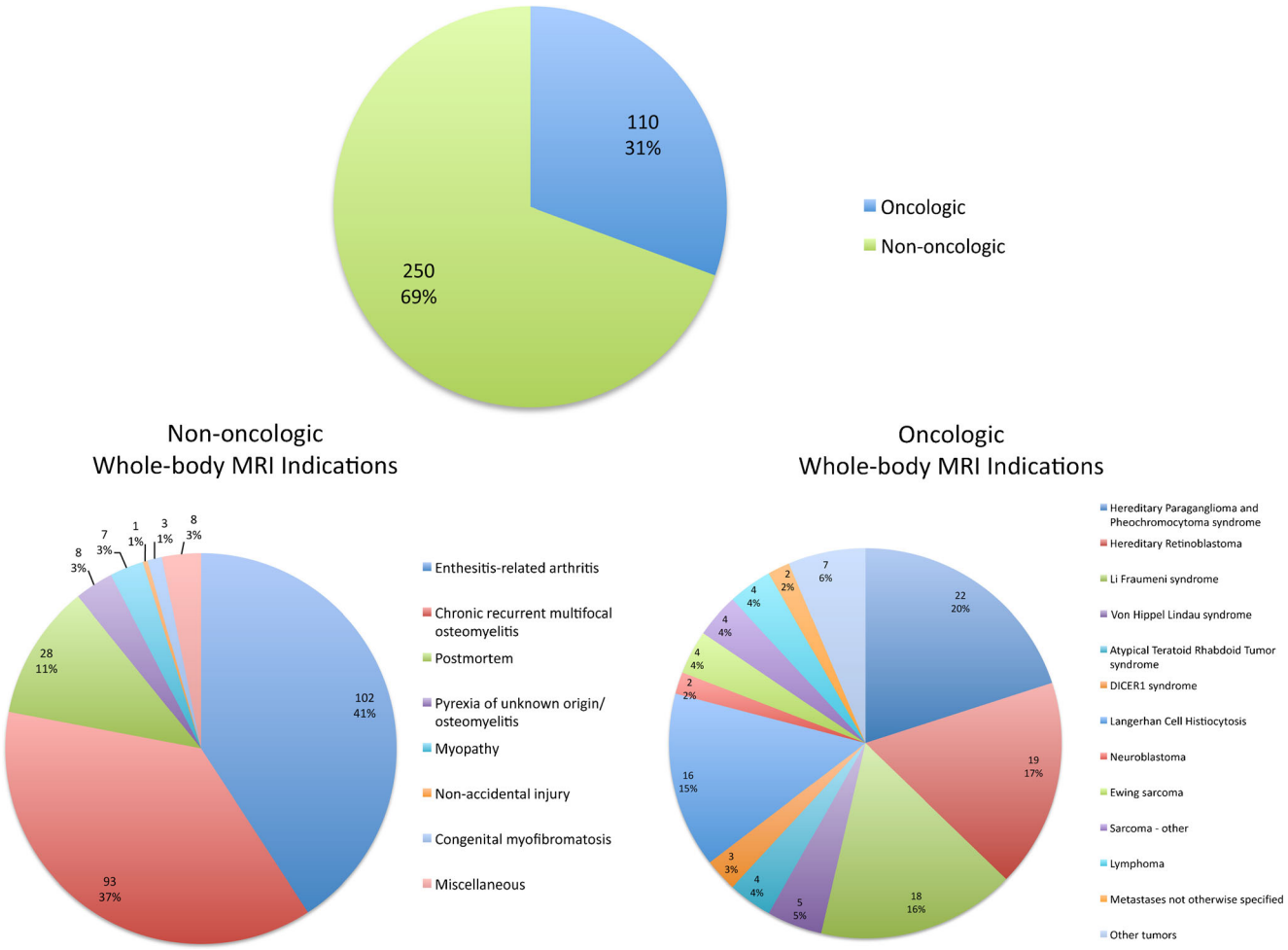

Fig. 2 Non-oncologic and oncologic whole-body MRI referrals over a 12-month period in 2017 at a single tertiary pediatric institution

indications. Imaging findings in a range of non-oncologic indications in infants, children and adolescents are then further described with whole-body MRI examples.

Whole-body magnetic resonance imaging technique

The general advantages of MRI are well known, as already discussed. Whole-body MRI additionally offers large FOV imaging, enabling wide coverage in a single examination. This needs to be balanced against limitations this imposes on spatial and contrast resolution, by extension size and signal of detectable lesions, as compared with smaller FOV regional imaging. Whether using whole-body MRI as a diagnostic tool in the work-up of a symptomatic child or for surveillance imaging, awareness of this impact on sensitivity and specificity can have important clinical implications. For many conditions, size thresholds for lesion detection in whole-body MRI are yet to be fully elucidated. Whole-body MRI has been shown to be superior to PET for osseous lesions <12 mm, but of lower sensitivity for lung lesions or lymph nodes less than 6 mm [3, 23]. To improve lesion detection in a subset of diseases, one- or two-plane large FOV imaging is complemented by focused imaging of sites more susceptible to disease-related pathology, as in ERA where the specific protocol includes whole-body MRI plus targeted imaging of the hips, knees, ankles, sacroiliac joints and spine [24]. As such, whole-body MRI protocols (Table 1) are integrally related to the indication, sequences and coverage adapted to the expected pathology [25].

Coverage and definitions

This introduces a key concept: what is meant by the term "whole-body MRI." Whole-body MRI is multiregional,

Table 1 Non-oncologic indication-specific whole-body MRI protocols from a single tertiary pediatric institution

Indication	Whole-body MRI planes and sequences	Supplementary targeted sequences	Optional sequences
ERA	Coronal STIR	Sagittal STIR spine Axial STIR pelvis Coronal oblique STIR sacroiliac joints Sagittal STIR bilateral knees & ankles	
CRMO	Coronal STIR	Sagittal STIR spine	Whole-body axial T1-W FSE, T2-W FSE FS or STIR
Osteomyelitis/ pyrexia of unknown origin	Coronal STIR		Whole-body or ROI: Coronal, axial T1-W FSE +/− GBCA with FS axial DWI, axial T2-W FSE FS or STIR, sagittal T2-W FSE FS
Neuromuscular inherited myopathy	Axial STIR & T1-W FSE[a]		Limited FOV only: Axial STIR & T1-W FSE iliac crests-to-knees[a]
Neuromuscular inflammatory myopathy - Juvenile dermatomyositis - Polymyositis	Limited FOV: Shoulder & pelvic girdles Axial STIR & T1-W FSE[b] Limited FOV: Upper & lower limbs to wrists/ankles Axial STIR & T1-W FSE[b]		
Avascular necrosis e.g., sickle cell disease	Coronal STIR & T1-W FSE		
Fat deposition/ storage diseases e.g., Gaucher disease	Coronal STIR & T1-W FSE Limited FOV: AP – whole-body MRI	Axial SSFSE & isotropic SSFP AP Coronal STIR & T1-W FSE femurs Coronal STIR & T1-W FSE tibiae/fibulae	
Postmortem	Limited FOV: CAP – whole-body MRI Coronal T2-W FSE FS, T1-W FSE Axial T2-W FSE FS, T1-W FSE	Heart: 3-D T2-W FSE FS Brain: regional imaging protocol	
Miscellaneous, e.g., Non-accidental Injury	Coronal STIR		

AP abdomen and pelvis, *CAP* chest, abdomen and pelvis, *CRMO* chronic recurrent multifocal osteomyelitis, *DWI* diffusion-weighted imaging, *ERA* enthesitis-related arthritis, *FOV* field-of-view (specified for truncated whole-body MRI), *FS* fat-suppressed, *FSE* fast spin echo, *GBCA* gadolinium-based contrast agent, *ROI* region of interest *SSFSE* single-shot fast spin echo, *STIR* short-tau inversion recovery, *T1-W* T1-weighted, *T2-W* T2-weighted, *3-D* three-dimensional, *Whole-body MRI* whole-body magnetic resonance imaging (vertex to heels)

[a] slice thickness = 5 mm with minimal gap = 0.5 mm

[b] slice thickness = 5 mm with wider gap = 15 mm

contiguous imaging of the entire body. The term whole-body MRI should be reserved for head-to-foot or vertex-to-heel imaging [3, 5, 6]. Where a smaller FOV is sufficient, whole-body MRI can be truncated and should be annotated accordingly [5]. In myopathies, coverage might be limited to the extremities. In the cancer predisposition syndrome hereditary paraganglioma and pheochromocytoma (HPP) syndrome, as lesions occur in the autonomic nervous system whole-body MRI can be limited to the neck and torso. This smaller FOV can therefore be defined as "NCAP whole-body MRI" (neck, chest, abdomen and pelvis whole-body MRI), or "CAP whole-body MRI" (chest, abdomen and pelvis whole-body MRI) when supplemented by a dedicated neck MRI [5, 26]. Dedicated imaging can be comprehensive, i.e. "regional MRI" as in the neck MRI in HPP syndrome, or limited to one or more sequences, i.e. "targeted MRI" as in ERA. Use of standardized terminology promotes better uniformity in image acquisition, assisting whole-body MRI comparison within and between institutions, potentially reducing scanning time by imaging the most relevant areas.

Whole-body magnetic resonance image acquisition

Most often acquired in the coronal plane, whole-body MRI consists of sequential imaging at each station along the z-axis, the number determined by patient height. These stations are stitched together to create a single large FOV image at each slice position, merged by vendor-specific automatic composure post-processing tools [6, 27] (Fig. 3).

Hardware and software considerations

Parallel imaging, multi-transmit technology and sliding table movement, without the need to reposition coils, all contributed to whole-body MRI becoming a robust clinical technique [5, 6, 25, 27]. Coil options vary among vendors and anatomical region, with multichannel multi-element receiver coils or phased-array body coils, surface and in-table, often in combination. For cranial imaging performed as part of whole-body MRI, at my institution either a dedicated head coil or a body coil is used depending on the vendor. Multiple surface coils provide improved signal and contrast-to-noise ratios as well as better spatial resolution than body coils alone [4, 25, 27]. Whole-body MRI is technically feasible at 1.5-T and 3-T field strengths, and although Mohan et al. [28] found image quality was better at 1.5 T than 3 T with fewer artifacts, 3 T was still considered adequate, supported by a recent review comparing whole-body MRI at 1.5 T and 3 T in neurofibromatosis [29]. Z-axis coverage is usually about 190–200 cm, and with use of table extenders this can marginally increase [23]. Continuous table movement, rather than the usual step-wise acquisition, will likely become more widely applied beyond vascular whole-body MRI, particularly when performed in conjunction

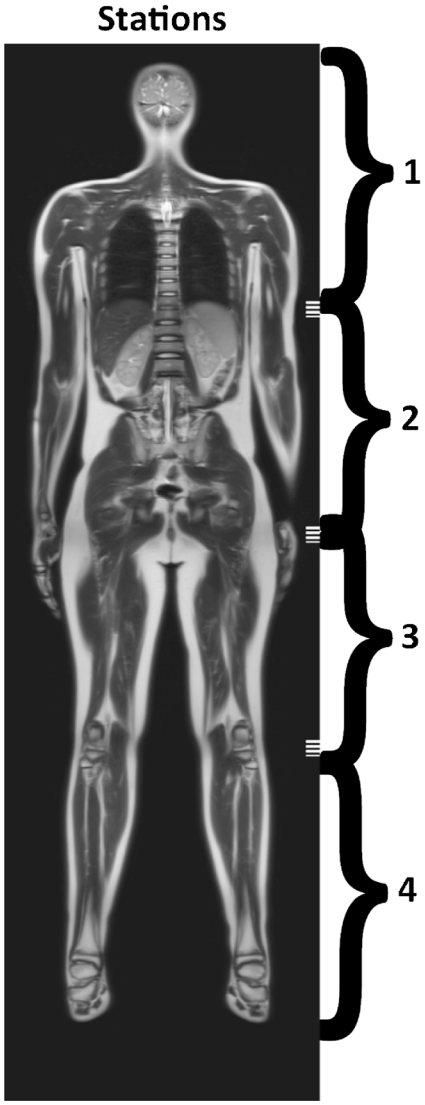

Fig. 3 Coronal single-shot T2-weighted scout MR image demonstrates stitching of four stations into a single coronal image, each station indicated by a curved bracket

with PET imaging, although image homogeneity and time gains can be offset by stair-step artifact and the large volume of data [27, 30, 31].

Sequences and imaging planes

While there is no standard whole-body MRI protocol, coronal short tau inversion recovery (STIR) is almost universally performed, providing anatomical information with pathological lesions typically bright, made more conspicuous by robust fat suppression [1, 5, 32]. Excellent for bone marrow and solid organ lesions, it is less sensitive for osteoblastic metastases. Institutional STIR sample parameters are: echo time/repetition time (TE/TR) 95/8,910 ms, matrix 384 × 384, FOV 500 mm, phase oversampling 25–30%, phase-encoding direction foot to head, slice thickness 5 mm and gap 1 mm. Average

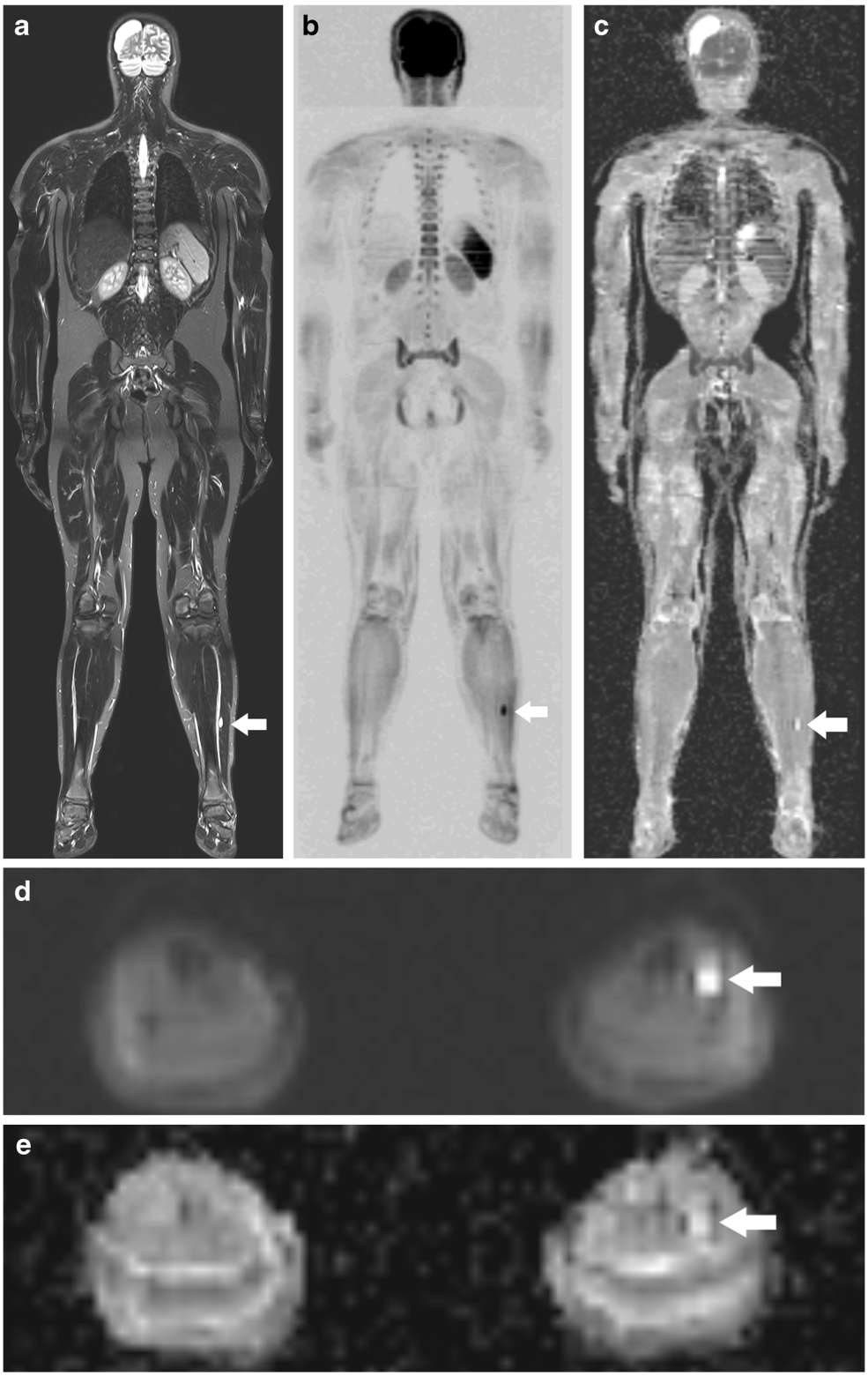

Fig. 4 Leg lesion post-resection of an atypical teratoid/rhabdoid tumor from the right parietal lobe in an 11-year-old boy. **a** Coronal short tau inversion recovery MRI. **b** Inverted diffusion-weighted image (DWI; b=800 s/mm^2). **c** Apparent diffusion coefficient (ADC) map. All show a lesion in the left calf (*arrows*). The calf lesion is most conspicuous in (**b**). Low signal on (**b**) and high signal on axial non-inverted DWI (**d**) and coronal (**c**) and axial (**e**) ADC maps are consistent with T2 shine-through in a non-restricting cystic lesion, of low clinical concern

acquisition time is 3 min 30 s per stack of 42–45 slices. Other anatomical sequences include T1-weighted fast spin echo (FSE), good for assessing bone marrow and solid organs; three-dimensional gradient echo sequences, and single-shot or steady-state free precessionT2-weighted imaging, which are also good for solid organs, and the latter sequences bowel and potentially lung imaging [1, 3, 4, 6, 23, 27]. These can be acquired with or without fat suppression. In- and opposed-phase sequences can be acquired independently or as part of the Dixon technique that offers homogeneous large FOV

suppression of water or fat signal in a single acquisition [27, 32, 33]. This can be applied to T1- or T2-weighted sequences. Gadolinium-based contrast agents (GBCAs) are seldom used in whole-body MRI, more so in regional imaging if contemporaneous, with increasing interest in ultra-small super-paramagnetic iron oxide particles (USPIO) to better evaluate the lymphoreticular system [34, 35]. Breath-holds are limited to less than 20 s for T1-weighted sequences, free-breathing for T2-weighted sequences, and electrocardiography (ECG) and respiratory triggering might be required in the chest, respiratory triggering in the upper abdomen.

Diffusion-weighted imaging (DWI) in whole-body MRI adds functional information, qualitative and quantitative if measuring apparent diffusion coefficient (ADC) values [7, 32, 36]. Along with increasing lesion conspicuity, DWI helps characterize lesions [7] (Fig. 4). DWIBS —or diffusion-weighted whole-body imaging with background suppression — is acquired free-breathing with fat suppression, using either CHESS (a chemical-shift selective imaging sequence) or SPIR (spectral presaturation with inversion recovery). Typically axial images are acquired and reconstructed in coronal plane to minimize artifacts, at slice thicknesses of 4–5 mm, matrix 128 × 128, and with a rectangular FOV. The number of excitations varies at each station to maintain a steady signal-to-noise ratio. At the author's institution we use b values of 0 s/mm^2, 50 s/mm^2 and 1,000 s/mm^2, ensuring at least one is ≤100 s/mm^2 to reveal the contribution of microcirculation to signal, with higher b values to characterize

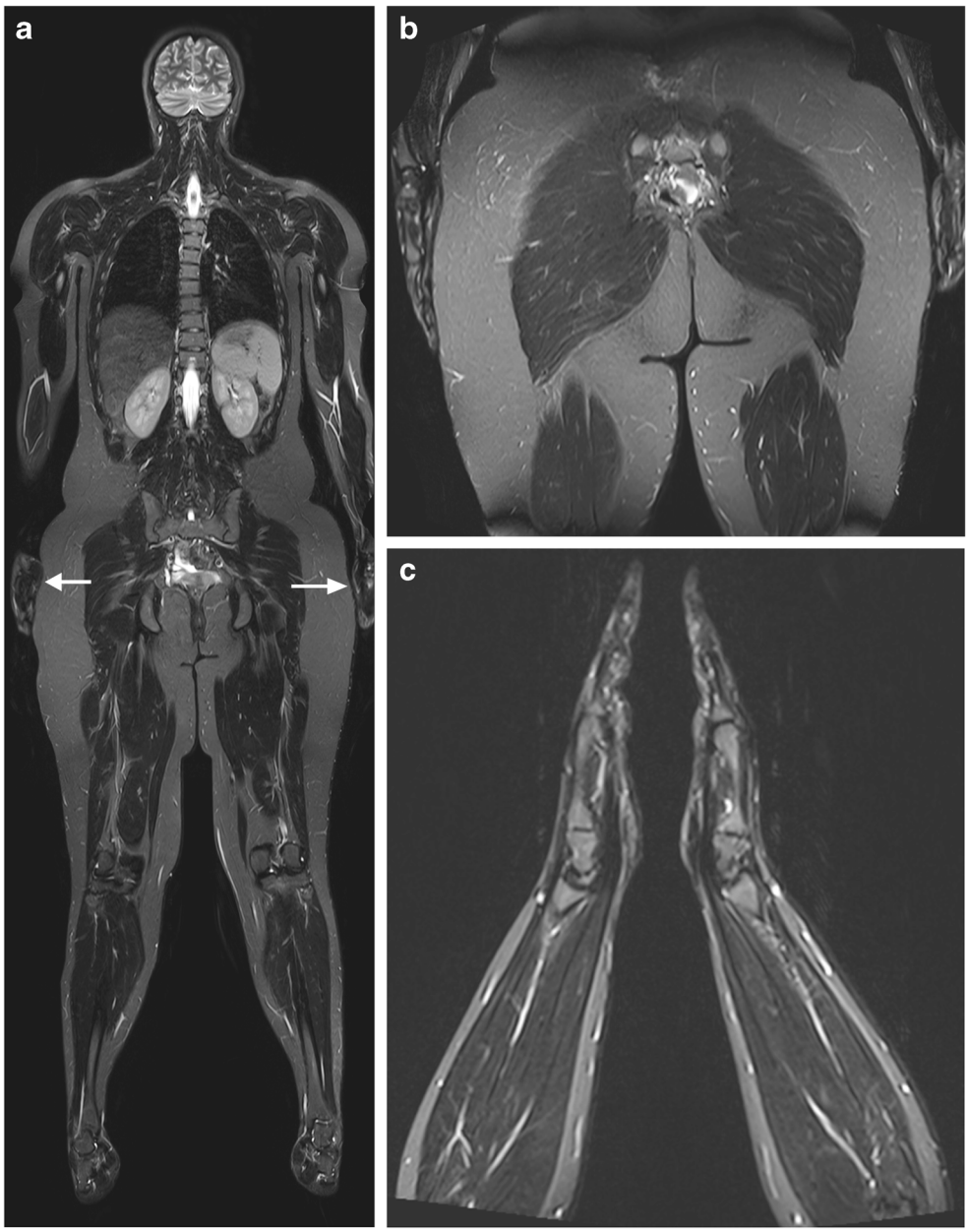

Fig. 5 Pitfalls. Coronal short tau inversion recovery MRI in a 17-year-old girl. **a** Whole-body MRI and (**b**) single-station MRI show partial cut-off of the girl's hands and forearms (*arrows*) when by her side, **c** The hands and arms are better visualized when scanned over her head

lesions [7, 25]. Acquisition times of 3 min 18 s per stack can be decreased to 1 min 42 s using multi-slice excitation. Images are inverted for display, mimicking a PET scan to aid analysis. We archive and analyze source axial DWI and ADC maps, coronal inverted DWI and coronal ADC maps. DWI adds value in tumor assessment, increasing sensitivity for lesion detection, with a lesser role in inflammatory conditions and osteonecrosis, and should be viewed in conjunction with anatomical sequences to improve specificity [7, 25, 37]. Further validation is warranted; however a recent pediatric study by Merlini et al. [38] compared 54 whole-body MRI protocols with and without DWI, showing similar sensitivities.

The coronal plane is most frequently employed in whole-body MRI for STIR and DWI, with sagittal and axial planes more variably acquired based on anticipated disease distribution. Imaging planes and sequences for non-oncologic whole-body MRI indications are summarized in Table 1.

Pitfalls

Pediatric patients are scanned supine, arms by their side, for greater comfort and less motion. Occasionally aliasing artifact occurs in larger children if their hands and forearms are far from the magnet isocenter, and this can be improved by obtaining an additional station with the child's arms temporarily overhead [14, 23] (Fig. 5). Stitch artifacts can occur where two stations are merged; signal loss from this can be minimized by phase oversampling (Fig. 6). Motion artifact can be more difficult to recognize on reconstructed images. Use of coronal imaging alone can limit detection of rib and sternal lesions, as well as lymph nodes depending on location. Nonspecific or false-positive findings can lead to unnecessary investigations.

Risks

On average, whole-body MRI acquisition times at our institution range 30–60 min, depending on the protocol. For patients 6 years or younger, sedation/general anesthesia is generally needed, although general anesthesia alternatives can be employed to minimize this need [5, 39, 40]. Small but real risks related to sedation, general anesthesia and GBCAs are beyond the scope of this manuscript.

Non-oncologic indications for whole-body MRI

The list of non-oncologic indications for whole-body MRI in the pediatric population continues to grow, with musculoskeletal conditions — rheumatologic diseases in particular — being the most common indication. This is similar in adults, although they have a slightly different spectrum of musculoskeletal disease, including psoriatic arthritis and ankylosing spondylitis

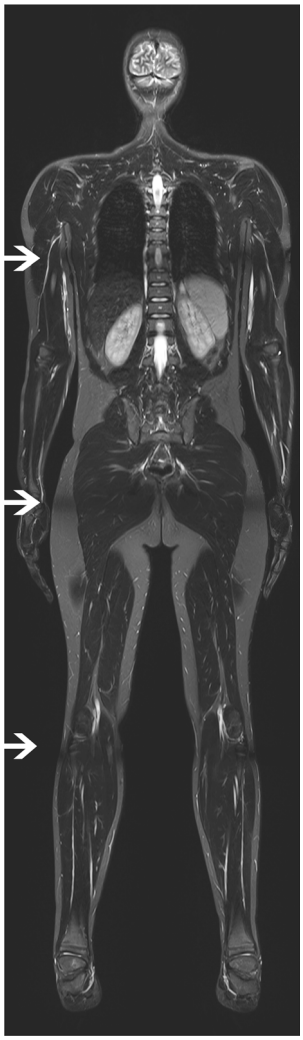

Fig. 6 Stitch artifact. Coronal short tau inversion recovery MRI in an 11-year-old boy. Arrows show faint signal loss where stations merge, a result of stitch artifact

[25, 41]. Whole-body MRI can be used to detect bone marrow, joint and soft-tissue lesions in ERA and CRMO to achieve a diagnosis, to define extent and treatment response, and to provide clues to disease activity [4]. In a retrospective study by Korchi et al. [41] of 42 non-oncologic children undergoing whole-body MRI, whole-body MRI was particularly helpful in confirming the diagnosis of CRMO and identifying the focus of pyrexia or arthralgia of unknown origin (PUO). Whole-body MRI can direct medical versus surgical management in clinically suspected osteomyelitis, particularly if it is multifocal or in younger children in whom it can be difficult to localize, and more rarely whole-body MRI is useful in diagnosing chronic granulomatous disorders and cysticercosis [3, 41].

In neuromuscular diseases, inflammatory and non-inflammatory, the pattern of muscle involvement on whole-body MRI can help define disease subtype, especially early on, and direct biopsy [18, 19]. Other indications include diagnosis and monitoring of avascular

necrosis (AVN) and storage disorders such as Gaucher disease, adipose tissue distribution, postmortem imaging, and skeletal dysplasias such as McCune-Albright syndrome and polyostotic fibrous dysplasia [3, 6, 27]. Whole-body MRI in non-accidental injury is controversial, considered to be of limited value, and is rarely performed [3, 23, 42]. A number of these diseases are reviewed next, illustrating the indication-specific whole-body MRI protocols summarized in Table 1.

Rheumatologic disorders

Whole-body MRI is now considered central to defining total inflammatory burden in children with arthritis [24, 25, 43]. Focusing on joints and entheses, evidence of synovitis, osteitis and soft-tissue inflammation on whole-body MRI form the basis of a proposed Outcome Measures in Rheumatology (OMERACT) scoring system, which also factors in severity of inflammation [43].

Enthesitis-related arthritis

An inflammatory arthritis of particular interest in children and adolescents, ERA is an HLA-B27-positive juvenile spondyloarthritis that primarily affects peripheral joints and entheses [24, 44]. Accounting for 20% of juvenile idiopathic arthritis, this affects more boys than girls, with mean age at diagnosis of 11.7 years [4, 24]. Lower-extremity joints are involved earliest; sacroiliac joints and the spine can be much later, with infrequent involvement of humeral tuberosities [4, 24]. The ERA-specific whole-body MRI protocol has been described (Table 1). Characteristic imaging findings are: *enthesitis* with T2-weighted hyperintense bone marrow edema, perienthesal soft-tissue swelling and edema, synovitis and joint/bursal fluid, commonly affecting the inferior pole of the patellar, ischial tuberosity, hip extensor insertion at the greater trochanter and plantar fascia insertion at the calcaneus; *arthritis* with bone marrow and soft-tissue edema, synovitis and joint/bursal fluid, e.g.,

Fig. 7 Enthesitis-related arthritis in a 15-year-old boy with back pain who is HLA-B27+. Short tau inversion recovery (STIR) MRI shows multifocal bone marrow STIR hyperintensities (*arrows*), in keeping with edema. **a** On coronal whole-body MRI, hyperintensities are seen in the right iliac bone and bilateral greater trochanters; *circles* show signal change in the distal femora and proximal tibiae. **b** Sagittal spine MRI shows edema at T4, T5 and T10–12, particularly the posterior extension into the pedicle at T5. **c** Coronal oblique MRI of the sacroiliac joints shows involvement in the right iliac ala and left lower sacral segments. **d** Sagittal image shows involvement of the left ankle at the anterior aspect of the periphyseal region of the distal tibia. **e** Axial image of the hips in the greater trochanters bilaterally and left ischial tuberosity and (**f**) sagittal image of the left knee in the epiphyses of the distal femur and proximal tibia both show involvement, as well

midfoot tarsitis in 33–88%; *sacroiliitis* with subchondral edema, joint/capsule edema and enhancement, and chronic erosions, sclerosis and finally ankylosis; and *corner lesions* of the vertebral endplates with bone marrow edema, osteitis or erosions, becoming fatty if chronic or healed ("fatty Romanus" sign) [4, 24, 25] (Fig. 7).

Chronic recurrent multifocal osteomyelitis

Chronic recurrent multifocal osteomyelitis (CRMO) is a non-bacterial autoinflammatory osteitis of unclear etiology that manifests clinically with pain and a restricted range of movement for more than 6 months [14, 45, 46]. More common in females, it has an incidence of 0.4/100,000 [45, 46]. Whole-body MRI has a pivotal role in the diagnosis of CRMO in children and adolescents, in whom it is most prevalent, and also in defining activity and treatment response, which often requires long-term imaging surveillance [4, 25, 47, 48]. In addition to coronal STIR whole-body MRI, a targeted sagittal STIR sequence of the whole spine is acquired (Table 1). Whole-body MRI facilitates detection of lesions in the following key sites: pelvis, femora, tibiae, ankles, feet, spine, clavicles, sternum and ribs. Multifocal and bilaterally symmetrical in 75% of cases, focal bone marrow lesions are characteristically perimetaphyseal, on one study in up to 90% [4, 14, 46, 48]. They are hyperintense to bone marrow, similar to or slightly less bright than fluid on STIR, and somewhat geographic and ill-defined [46]. Other CRMO imaging features can include juxtaphyseal nodules, periosseous edema, myositis, synovitis, joint effusions, and vertebra plana [4, 14, 48]. While not currently performing DWI for CRMO at our center, if there is concern regarding malignancy, high ADC values in CRMO lesions have been shown to be a useful discriminator relative to lower ADC values in tumors [49] (Fig. 8).

Infections

In the very young and immune-suppressed, localizing a source of sepsis can be challenging [3, 14]. Whether it

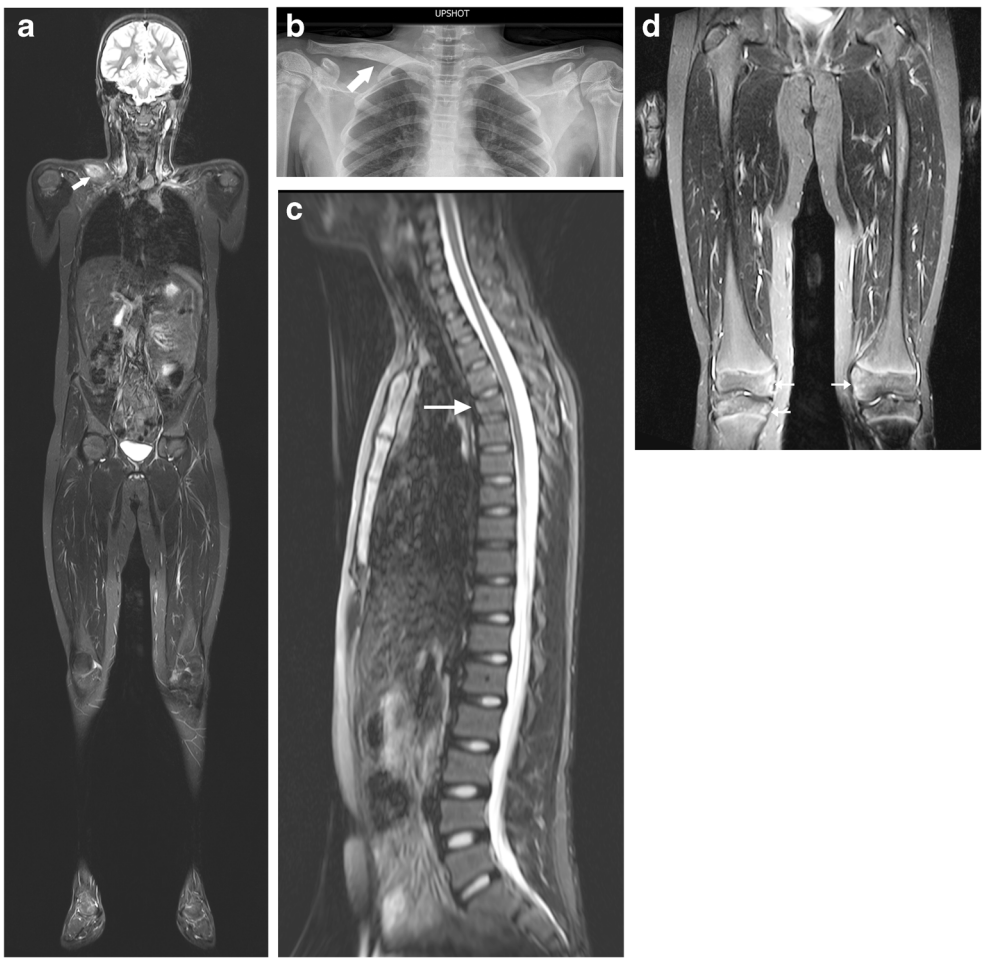

Fig. 8 Chronic recurrent multifocal osteomyelitis (CRMO) in an 11-year-old boy. **a** Coronal short tau inversion recovery (STIR) whole-body MRI and (**b**) clavicle radiograph show expansion of the right anteroposterior clavicle. MRI shows increased bone marrow signal and peri-osseous soft-tissue edema (*arrow*). **c** Sagittal STIR spine MRI shows T5 vertebra plana (*arrow*). **d** Single station of the lower extremities from the coronal STIR whole-body MRI shows bilateral distal femoral and right proximal tibial epiphyseal and perimetaphyseal asymmetrical ill-defined hyperintense lesions (*arrows*)

is suspected to originate from the musculoskeletal system, as in osteomyelitis and septic arthritis, an extra-osseous site, or undefined as in pyrexia of unknown origin (PUO) with the differential ranging from abscess to malignancy, the wide coverage and exquisite soft-tissue detail in whole-body MRI can lead to the diagnosis [14, 41]. Whole-body MRI can also define the number and sites of disease if multifocal, direct therapy (e.g., percutaneous subperiosteal abscess drainage versus antibiotics alone) and monitor response, all without ionizing radiation [3, 23]. The whole-body MRI technique for osteomyelitis and PUO is a blend of generic and lesion-specific imaging. Coronal whole-body STIR is again standardly acquired and might be sufficient to exclude pathology. However if warranted, targeted imaging with the plane and sequence choices tailored to regions of interest can be guided by patient symptoms or findings on the initial STIR whole-body MRI acquisition (Table 1).

Osteomyelitis can present as ill-defined areas of bone marrow T2-weighted hyperintensity with enhancement if using GBCAs, or more discrete intra-osseous or subperiosteal fluid collections with low to intermediate signal on T1- and intermediate to high signal on fat-suppressed T2-weighted sequences, centrally restricting on DWI, and rim-enhancing. Whole-body MRI can also reveal intramuscular abscesses; necrotizing fasciitis; myositis with patchy or diffuse T2-weighted hyperintensity and enhancement; septic arthritis — joint fluid with synovial thickening or enhancement, although nonspecific; and anasarca [14, 23, 41] (Fig. 9). Whole-body

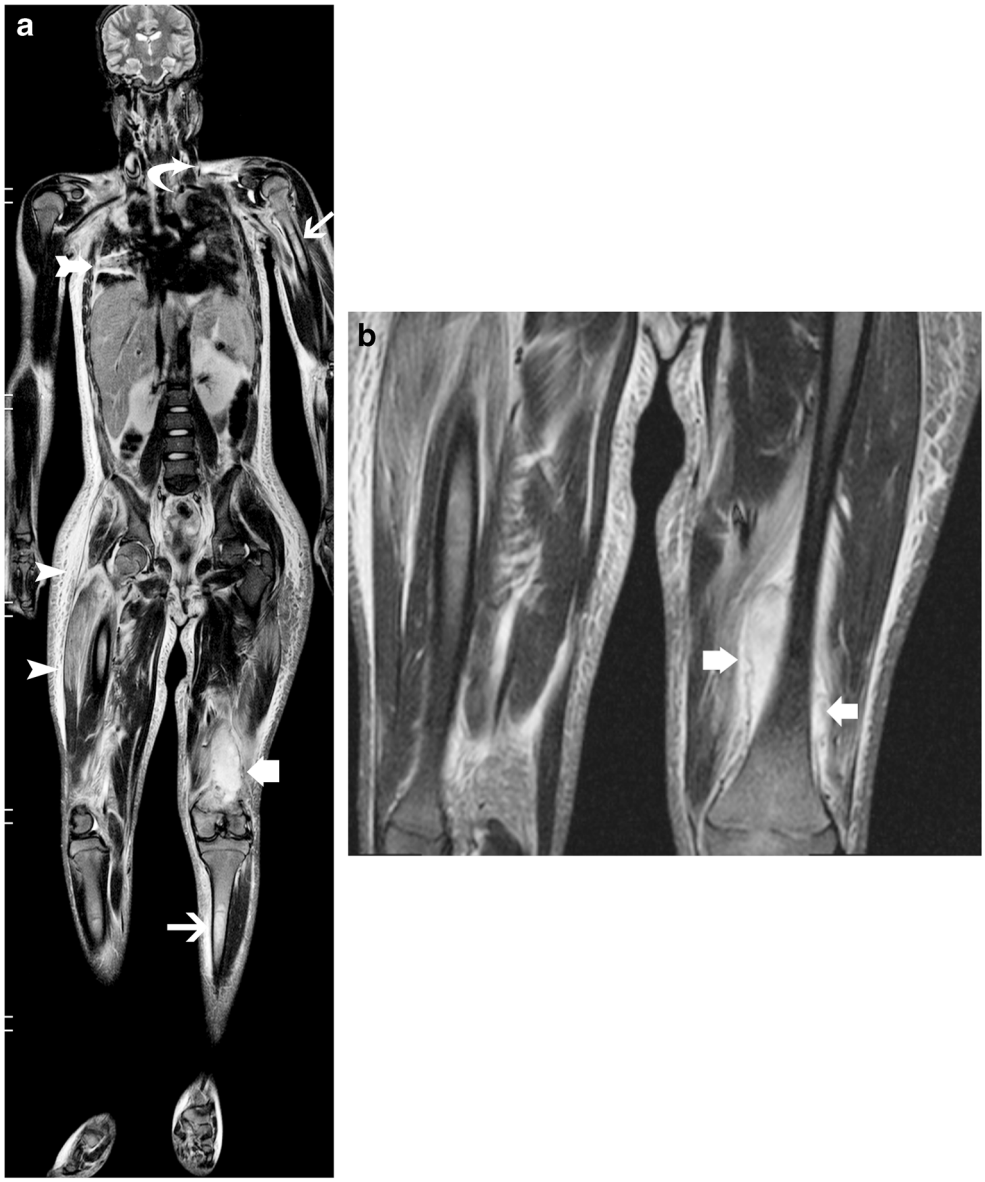

Fig. 9 Infection. **a** Coronal short tau inversion recovery whole-body MRI and (**b**) expanded single-station images from the lower extremities in a 10-year-old girl with disseminated *Staphylococcus aureus* infection. Findings include osteomyelitis in the left humerus and left tibia (*thin arrows*), a subperiosteal abscess in the left distal femur (*thick arrows*), a left supraclavicular fossa inflammatory mass (*curved arrow*), diffuse myositis and anasarca in the right thigh (*arrowheads*) and pleural fluid with consolidation/collapse in the right lung (*double-headed arrow*), with septic pulmonary emboli (not shown)

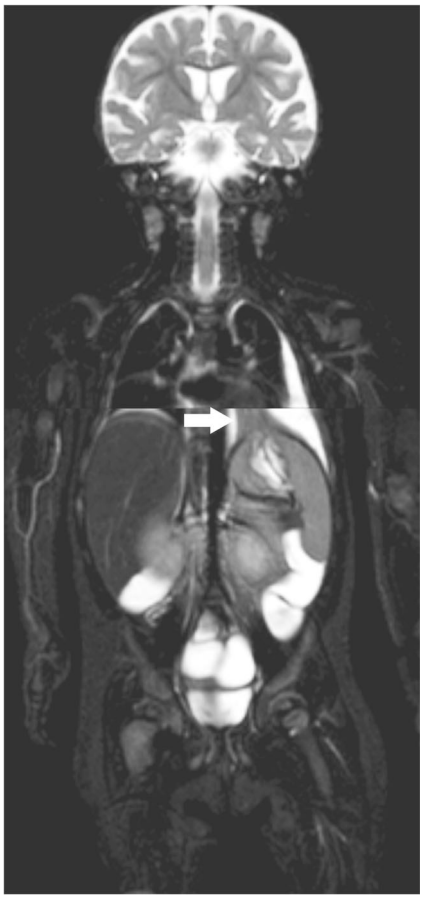

Fig. 10 Pyrexia of unknown origin in a 7-month-old girl with 8 days of fever. Coronal short tau inversion recovery (STIR) truncated whole-body MRI from vertex to thighs (mismatch in merged images resulting from patient movement between station acquisitions) reveals left lower lobe pneumonia and a pleural effusion (*arrow*). Interestingly, the chest radiograph was normal on admission 1 week prior

MRI can depict non-musculoskeletal sources including solid organ abscesses, pneumonia and septic pulmonary emboli [14, 23, 41] (Figs. 9 and 10).

Neuromuscular disorders

Inherited myopathies

Whole-body MRI is invaluable in assessing early onset neuromuscular disorders manifesting as muscle weakness, including muscular dystrophies, congenital myopathies and spinal muscular atrophy, and for screening relatives [3, 18]. Through faster techniques, comprehensive imaging of individual muscles and muscle groups in the head and neck, torso, shoulder and pelvic girdles, and upper and lower limbs is now feasible. Whole-body MRI demonstrates increased signal intensity on T2-weighted imaging in affected muscles with active disease, muscle atrophy with fatty infiltration when chronic, altered subcutaneous fat distribution on T1-weighted sequences, and different patterns of involvement and severity, so whole-body MRI can be instrumental in diagnosing specific inherited myopathies, as detailed by Quijano-Roy et al. [18]. Further, whole-body MRI can distinguish active and chronic disease and direct biopsy [3, 25] (Fig. 11). Use of contiguous small gap axial sequences allows better definition of the muscle groups for anatomical mapping and volume assessment on T1-weighted imaging, and intramuscular edema, necrosis or inflammation on STIR, enabling qualitative and increasingly quantitative assessment [19] (Table 1).

Inflammatory myopathies

Juvenile dermatomyositis and polymyositis are idiopathic inflammatory myopathies. Prompt diagnosis and treatment is crucial for improved outcomes, especially in juvenile dermatomyositis, where whole-body MRI can define inflammatory disease burden [3, 14, 50]. Presenting with symmetrical, proximal greater than distal muscle weakness, they are characterized by muscular and subcutaneous inflammatory lesions, as well as extramuscular lesions. In a study by Huang et al. [51] of 129 children and adults undergoing whole-body MRI, extramuscular lesions included interstitial lung disease in 29.5%; neoplasia in 9.3%, including two cases of nasopharyngeal carcinoma; and post-steroid therapy osteonecrosis in 15% [14]. Whole-body MRI technique can be truncated and non-contiguous, but juvenile dermatomyositis and polymyositis are multifocal, qualifying them for consideration in whole-body MRI disorders.

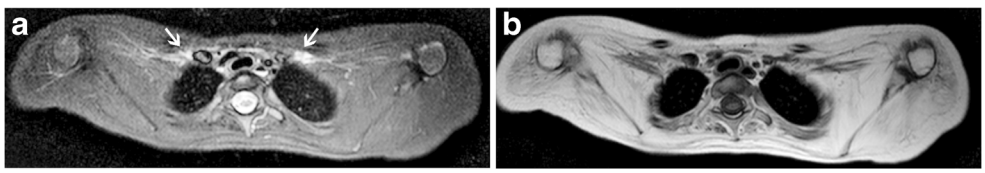

Fig. 11 Inherited myopathy in a 9-year-old girl with inactive, chronic severe myositis, with progressive muscle weakness since 2 years old. **a** Axial short tau inversion recovery (STIR) MRI shows minimal edema in severely atrophic pectoral muscles (*arrows*). **b** Axial T1-weighted turbo spin-echo sequence shows bilaterally symmetrical proximal muscular atrophy and fatty deposition in shoulder girdle and paraspinal muscles

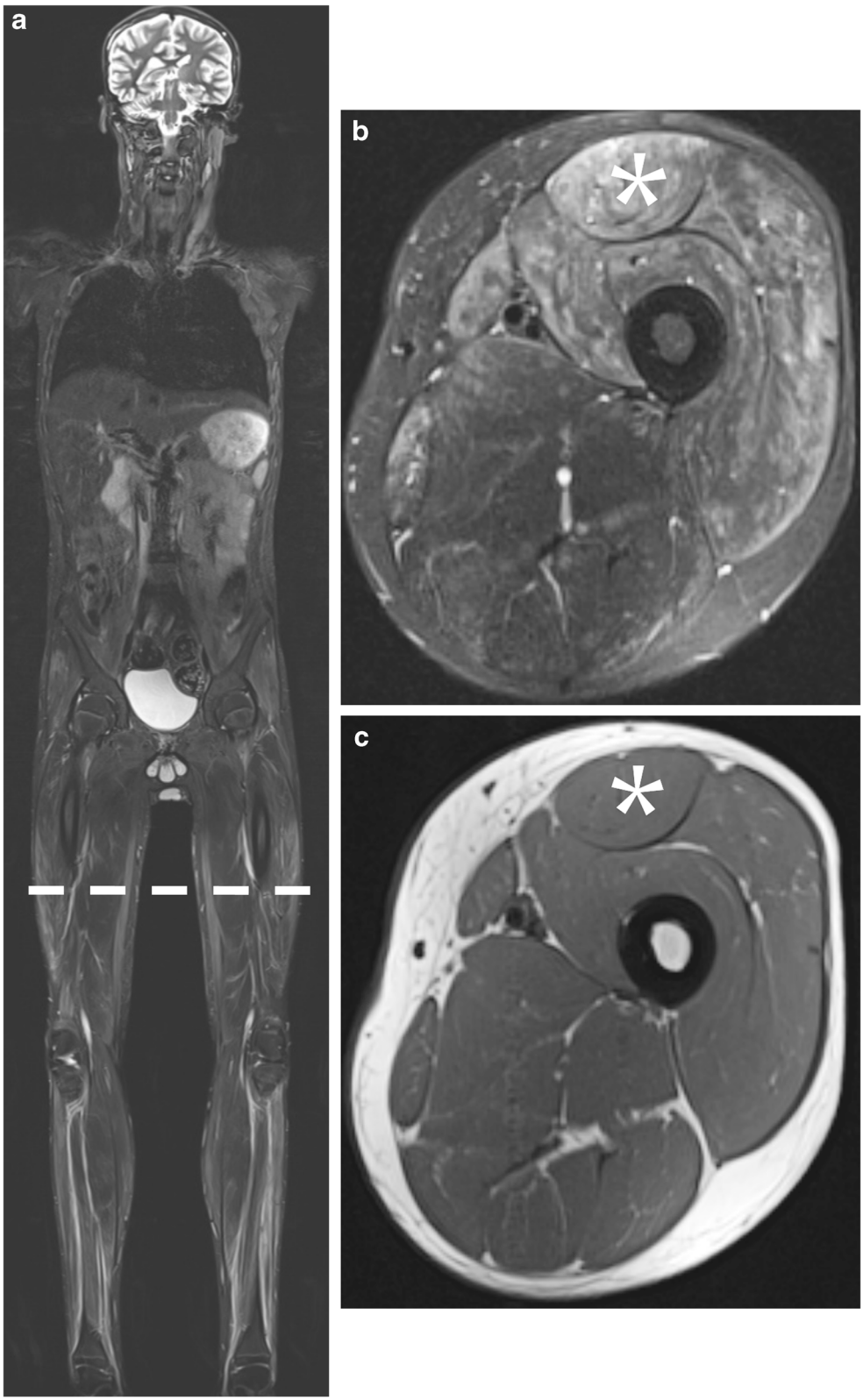

Fig. 12 Inflammatory myopathy in a 12-year-old boy with new-onset muscle weakness who was diagnosed with juvenile dermatomyositis. **a** Coronal short tau inversion recovery (STIR) whole-body MRI allows localization of axial sequences (indicated by *dashed line*). Active disease is evidenced by bilaterally symmetrical muscle and subcutaneous edema in the lower extremity. **b** Axial STIR MRI (**b)** shows patchy, diffuse T2-weighted hyperintense muscle and myofascial edema maximal in the anterior compartment, in particular the rectus femorus muscle (*). **c** This is of normal signal without fat or atrophy on axial T1-weighted MRI (*)

Coverage can be limited to the shoulder and pelvic girdles or the entire upper and lower extremities, employing wider gaps than for inherited myopathies (Table 1). STIR hyperintensities reflect edema and inflammation in muscles and in myofascial and subcutaneous tissues; T1 hyperintensity shows intramuscular fat deposition

— similarly in juvenile dermatomyositis and polymyositis, except that subcutaneous involvement is more common in juvenile dermatomyositis [3, 14, 51] (Fig. 12).

Avascular necrosis

Avascular necrosis (AVN), or osteonecrosis, and bone infarcts can be multifocal, affecting the axial and appendicular skeleton, especially epiphyses of weight-bearing joints and vertebrae, e.g., in sickle cell disease (SCD) [25, 52]. In addition to occurring in hypercoagulable states such as SCD, high-dose corticosteroid therapy poses a particular risk, with AVN increasingly recognized on whole-body MRI in diseases such as juvenile dermatomyositis and polymyositis or Hodgkin lymphoma [50, 51, 53]. The combination of coronal STIR and T1-weighted sequences allows for detection of these lesions. They are typically seen as well-defined geographic areas of abnormal marrow signal demarcated peripherally by a characteristic rim of high signal on STIR and low signal on T1, sometimes with articular surface collapse, with imaging helping estimate the percentage of involvement of an affected bone such as the femoral head [50, 51] (Table 1). DWI has been suggested in SCD but is not routinely performed on whole-body MRI for AVN at our institution [52].

Fat deposition and storage disorders

Coronal T1-weighted whole-body MRI, alone or in combination with STIR, can be used to demonstrate adipose tissue deposition and distribution in familial lipodystrophies, e.g., neonatal progeroid syndrome, to localize sites of rapid loss of subcutaneous fat, or increase in lipomatosis syndromes or in bariatric patients [3, 54] (Fig. 13). It can be of value in storage disorders such as Gaucher disease, a disorder in which AVN can also occur. Whole-body MRI is supplemented by targeted MRI of the abdomen, which is beneficial when calculating abdominal adipose tissue relative to skeletal muscle as in Prader–Willi syndrome [3, 55] (Table 1).

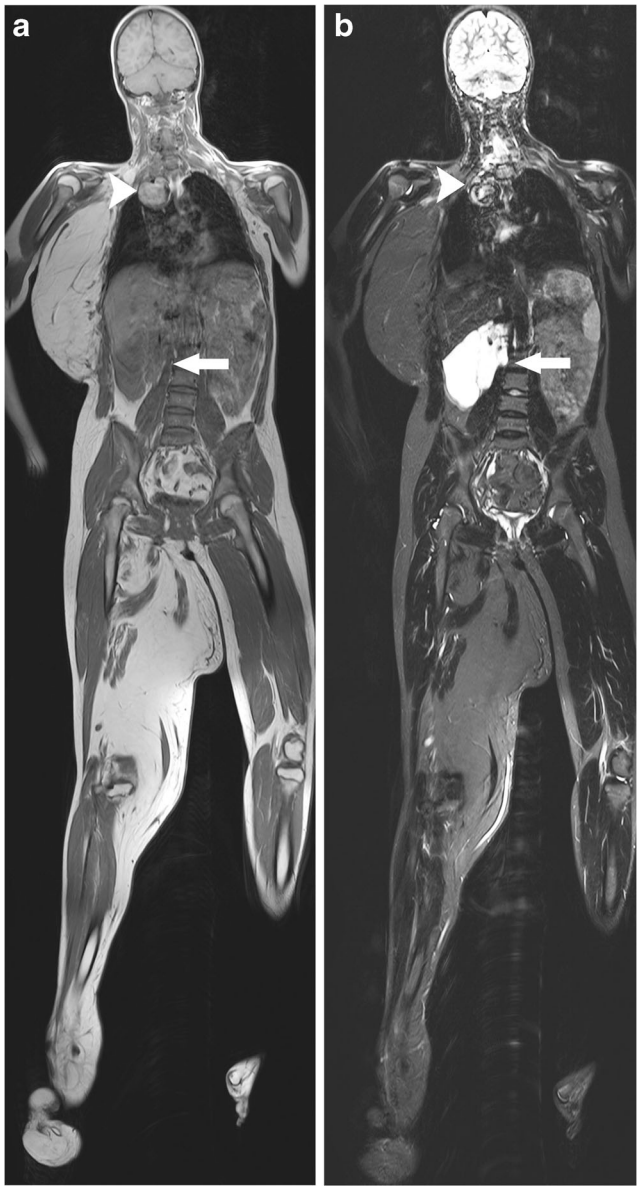

Fig. 13 Lipomatosis syndrome in a 12-year-old girl with chronic asymmetrical increase in adipose tissue, most marked in the right hemithorax and right thigh, best demonstrated on (**a**) coronal T1-weighted whole-body MRI. **b** Coronal short tau inversion recovery (STIR) whole-body MRI demonstrates additional pathology — uncomplicated retroperitoneal (*arrow*) and hemorrhagic mediastinal lymphatic malformations (*arrowhead*), respectively, of low and intermediate signal on (**a**) and high and heterogeneous signal on (**b**)

Postmortem

There has been a rapid expansion in cross-sectional whole-body postmortem imaging, in particular MRI, for reasons already considered, with target populations, standardization of imaging protocols, and impact yet to be established [20, 56]. Initial studies have shown a high concordance of postmortem MRI findings with conventional autopsy in fetuses, neonates and infants, and a preference by families for virtual over conventional autopsy [22, 57]. Table 1 summarizes our institutional postmortem MRI protocol, with whole-body MRI limited to the chest, abdomen and pelvis; targeted imaging of the heart; and separate regional brain MRI. Best for pathology in the central nervous system and least sensitive for lung abnormalities, familiarity with the spectrum of artifacts and normal postmortem MRI findings — including subcutaneous edema, small pleural and pericardial effusions and intravascular and hepatobiliary gas — is needed to optimize interpretation [21]. Knowledge of perimortem events such as resuscitation is also important (Fig. 14).

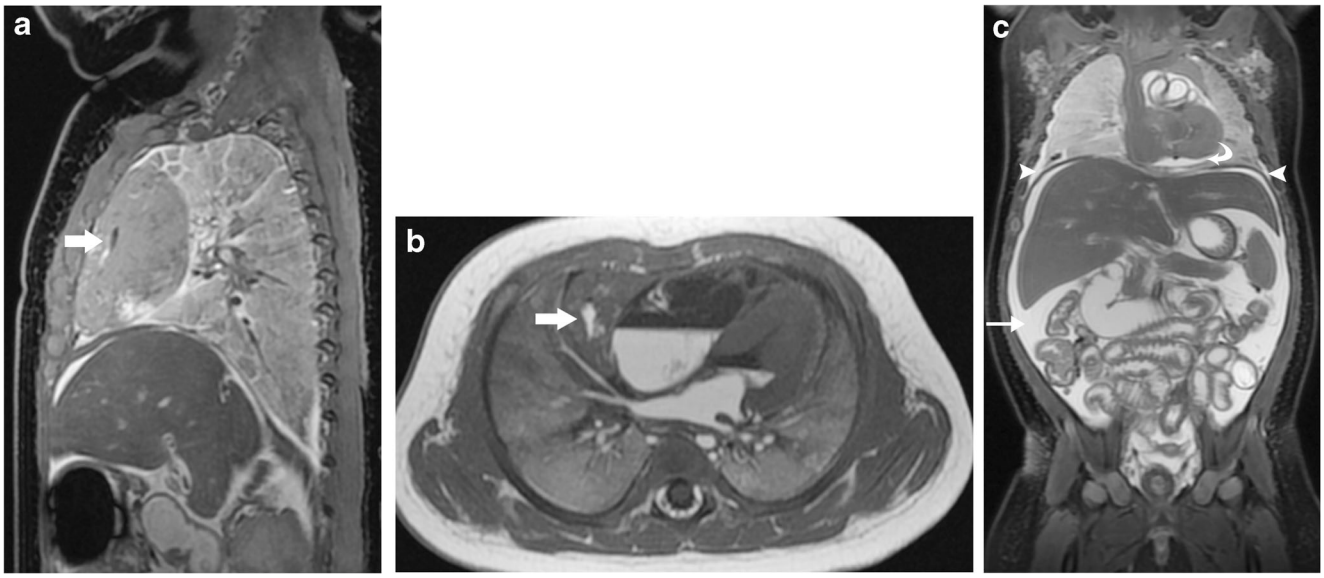

Fig. 14 Postmortem MRI in a 3-month-old girl who was found prone in crib, dusky and vomiting after a feed, aggressively resuscitated on transfer to an emergency department, with no cause of death identified on MRI or autopsy. **a** Sagittal T2-weighted turbo spin-echo (TSE) fat-suppressed image and (**b**) axial T1-weighted TSE image show a thymic hematoma (*arrow*). Bilateral anterolateral 2nd to 4th rib fractures were found only on autopsy, not evident on MRI, with the thymic hematoma confirmed at autopsy deep to the sternum. **c** Coronal T2-weighted TSE shows small amounts of pleural (*arrowheads*) and pericardial fluid (*curved arrow*) and a moderate amount of peritoneal fluid (*straight arrow*), the lungs with homogeneous increased signal (intermediate signal on T1-weighted image in **b**). At autopsy, the peritoneal fluid was serous (100 mL) and lungs edematous with no consolidation (combined weight 124 g, normal 89±23 g). These findings were also considered secondary to aggressive resuscitation. Fluid-fluid levels in the heart and great vessels and mild dilatation of bowel loops are common findings on postmortem MRI and not considered pathological

Conclusion

In whole-body MRI, the range of indications is matched by a plethora of different protocols, but standardized protocols based on specific indications can optimize interpretation for initial diagnosis and follow-up in defining the presence and extent of disease and treatment response. However it should be noted that even the simplest whole-body MRI technique using a single coronal STIR sequence can provide information that influences the care of pediatric patients.

Acknowledgments I thank Govind Chavhan, Andrea Doria, Jennifer Stimec, Manoj Singh, Sumeet Gupta, Tammy Rayner and Ruth Weiss for their contributions developing whole-body MRI at the Hospital for Sick Children, and Warren Corber for his assistance with the clinical audit.

Compliance with ethical standards

Conflicts of interest None

References

1. Ley S, Ley-Zaporozhan J, Schenk JP (2009) Whole-body MRI in the pediatric patient. Eur J Radiol 70:442–451
2. Atkin KL, Ditchfield MR (2014) The role of whole-body MRI in pediatric oncology. J Pediatr Hematol Oncol 36:342–352
3. Davis JT, Kwatra N, Schooler GR (2016) Pediatric whole-body MRI: a review of current imaging techniques and clinical applications. J Magn Reson Imaging 44:783–793
4. Eutsler EP, Khanna G (2016) Whole-body magnetic resonance imaging in children: technique and clinical applications. Pediatr Radiol 46:858–872
5. Greer MC, Voss SD, States LJ (2017) Pediatric cancer predisposition imaging: focus on whole-body MRI. Clin Cancer Res 23:e6–e13
6. Chavhan GB, Babyn PS (2011) Whole-body MR imaging in children: principles, technique, current applications, and future directions. Radiographics 31:1757–1772
7. Attariwala R, Picker W (2013) Whole body MRI: improved lesion detection and characterization with diffusion weighted techniques. J Magn Reson Imaging 38:253–268
8. Brenner DJ, Shuryak I, Einstein AJ (2011) Impact of reduced patient life expectancy on potential cancer risks from radiologic imaging. Radiology 261:193–198
9. Brady Z, Ramanauskas F, Cain TM et al (2012) Assessment of paediatric CT dose indicators for the purpose of optimisation. Br J Radiol 85:1488–1498
10. Goo HW, Choi SH, Ghim T et al (2005) Whole-body MRI of paediatric malignant tumours: comparison with conventional oncological imaging methods. Pediatr Radiol 35:766–773
11. Kanda T, Ishii K, Kawaguchi H et al (2014) High signal intensity in the dentate nucleus and globus pallidus on unenhanced T1-weighted MR images: relationship with increasing cumulative dose of a gadolinium-based contrast material. Radiology 270:834–841
12. Hu HH, Pokorney A, Towbin RB et al (2016) Increased signal intensities in the dentate nucleus and globus pallidus on unenhanced T1-weighted images: evidence in children undergoing multiple gadolinium MRI exams. Pediatr Radiol 46:1590–1598
13. Flood TF, Stence NV, Maloney JA et al (2017) Pediatric brain: repeated exposure to linear gadolinium-based contrast material is

associated with increased signal intensity at unenhanced T1-weighted MR imaging. Radiology 282:222–228
14. Damasio MB, Magnaguagno F, Stagnaro G (2016) Whole-body MRI: non-oncological applications in paediatrics. Radiol Med 121:454–461
15. van Engelen K, Villani A, Wasserman JD et al (2017) DICER1 syndrome: approach to testing and management at a large pediatric tertiary care center. Pediatr Blood Cancer 65(1)
16. Schultz KAP, Rednam SP, Kamihara J et al (2017) PTEN, DICER1, FH, and their associated tumor susceptibility syndromes: clinical features, genetics, and surveillance recommendations in childhood. Clin Cancer Res 23:e76–e82
17. Bueno MT, Martinez-Rios C, la Puente Gregorio A et al (2017) Pediatric imaging in DICER1 syndrome. Pediatr Radiol 47:1292–1301
18. Quijano-Roy S, Avila-Smirnow D, Carlier RY et al (2012) Whole body muscle MRI protocol: pattern recognition in early onset NM disorders. Neuromuscul Disord 22:S68–S84
19. Hollingsworth KG, de Sousa PL, Straub V et al (2012) Towards harmonization of protocols for MRI outcome measures in skeletal muscle studies: consensus recommendations from two TREAT-NMD NMR workshops, 2 may 2010, Stockholm, Sweden, 1-2 October 2009, Paris, France. Neuromuscul Disord 22:S54–S67
20. Arthurs OJ, van Rijn RR, Whitby EH et al (2016) ESPR postmortem imaging task force: where we begin. Pediatr Radiol 46:1363–1369
21. Arthurs OJ, Guy A, Thayyil S et al (2016) Comparison of diagnostic performance for perinatal and paediatric post-mortem imaging: CT versus MRI. Eur Radiol 26:2327–2336
22. Thayyil S, Sebire NJ, Chitty LS et al (2013) Post-mortem MRI versus conventional autopsy in fetuses and children: a prospective validation study. Lancet 382:223–233
23. Teixeira SR, Elias Junior J, Nogueira-Barbosa MH et al (2015) Whole-body magnetic resonance imaging in children: state of the art. Radiol Bras 48:111–120
24. Aquino MR, Tse SM, Gupta S et al (2015) Whole-body MRI of juvenile spondyloarthritis: protocols and pictorial review of characteristic patterns. Pediatr Radiol 45:754–762
25. Lecouvet FE (2016) Whole-body MR imaging: musculoskeletal applications. Radiology 279:345–365
26. Rednam SP, Erez A, Druker H et al (2017) Von Hippel-Lindau and hereditary pheochromocytoma/paraganglioma syndromes: clinical features, genetics, and surveillance recommendations in childhood. Clin Cancer Res 23:e68–e75
27. Goo HW (2015) Whole-body MRI in children: current imaging techniques and clinical applications. Korean J Radiol 16:973–985
28. Mohan S, Moineddin R, Chavhan GB (2015) Pediatric whole-body magnetic resonance imaging: intra-individual comparison of technical quality, artifacts, and fixed structure visibility at 1.5 and 3 T. Indian J Radiol Imaging 25:353–358
29. Ahlawat S, Fayad LM, Khan MS et al (2016) Current whole-body MRI applications in the neurofibromatoses: NF1, NF2, and schwannomatosis. Neurology 87:S31–S39
30. Weckbach S, Michaely HJ, Stemmer A et al (2010) Comparison of a new whole-body continuous-table-movement protocol versus a standard whole-body MR protocol for the assessment of multiple myeloma. Eur Radiol 20:2907–2916
31. Lindemann ME, Oehmigen M, Blumhagen JO et al (2017) MR-based truncation and attenuation correction in integrated PET/MR hybrid imaging using HUGE with continuous table motion. Med Phys 44:4559–4572
32. Morone M, Bali MA, Tunariu N et al (2017) Whole-body MRI: current applications in oncology. AJR Am J Roentgenol 209: W336–W349
33. Costelloe CM, Madewell JE, Kundra V et al (2013) Conspicuity of bone metastases on fast Dixon-based multisequence whole-body MRI: clinical utility per sequence. Magn Reson Imaging 31:669–675
34. Klenk C, Gawande R, Uslu L et al (2014) Ionising radiation-free whole-body MRI versus (18)F-fluorodeoxyglucose PET/CT scans for children and young adults with cancer: a prospective, non-randomised, single-centre study. Lancet Oncol 15:275–285
35. Finn JP, Nguyen KL, Hu P (2017) Ferumoxytol vs. gadolinium agents for contrast-enhanced MRI: thoughts on evolving indications, risks, and benefits. J Magn Reson Imaging 46:919–923
36. Nievelstein RA, Littooij AS (2016) Whole-body MRI in paediatric oncology. Radiol Med 121:442–453
37. Jaramillo D (2010) Whole-body MR imaging, bone diffusion imaging: how and why? Pediatr Radiol 40:978–984
38. Merlini L, Carpentier M, Ferrey S et al (2017) Whole-body MRI in children: would a 3D STIR sequence alone be sufficient for investigating common paediatric conditions? A comparative study. Eur J Radiol 88:155–162
39. Carter AJ, Greer ML, Gray SE et al (2010) Mock MRI: reducing the need for anaesthesia in children. Pediatr Radiol 40:1368–1374
40. Jaimes C, Gee MS (2016) Strategies to minimize sedation in pediatric body magnetic resonance imaging. Pediatr Radiol 46:916–927
41. Korchi AM, Hanquinet S, Anooshiravani M et al (2014) Whole-body magnetic resonance imaging: an essential tool for diagnosis and work up of non-oncological systemic diseases in children. Minerva Pediatr 66:169–176
42. Perez-Rossello JM, Connolly SA, Newton AW et al (2010) Whole-body MRI in suspected infant abuse. AJR Am J Roentgenol 195: 744–750
43. Ostergaard M, Eshed I, Althoff CE et al (2017) Whole-body magnetic resonance imaging in inflammatory arthritis: systematic literature review and first steps toward standardization and an OMERACT scoring system. J Rheumatol 44: 1699–1705
44. Weiss PF (2016) Update on enthesitis-related arthritis. Curr Opin Rheumatol 28:530–536
45. Arnoldi AP, Schlett CL, Douis H et al (2017) Whole-body MRI in patients with non-bacterial osteitis: radiological findings and correlation with clinical data. Eur Radiol 27:2391–2399
46. von Kalle T, Heim N, Hospach T et al (2013) Typical patterns of bone involvement in whole-body MRI of patients with chronic recurrent multifocal osteomyelitis (CRMO). Rofo 185:655–661
47. Voit AM, Arnoldi AP, Douis H et al (2015) Whole-body magnetic resonance imaging in chronic recurrent multifocal osteomyelitis: clinical longterm assessment may underestimate activity. J Rheumatol 42:1455–1462
48. Falip C, Alison M, Boutry N et al (2013) Chronic recurrent multifocal osteomyelitis (CRMO): a longitudinal case series review. Pediatr Radiol 43:355–375
49. Leclair N, Thormer G, Sorge I et al (2016) Whole-body diffusion-weighted imaging in chronic recurrent multifocal osteomyelitis in children. PLoS One 11:e0147523
50. Zhen-Guo H, Min-Xing Y, Xiao-Liang C et al (2017) Value of whole-body magnetic resonance imaging for screening multifocal osteonecrosis in patients with polymyositis/dermatomyositis. Br J Radiol 90:20160780
51. Huang ZG, Gao BX, Chen H et al (2017) An efficacy analysis of whole-body magnetic resonance imaging in the diagnosis and follow-up of polymyositis and dermatomyositis. PLoS One 12: e0181069
52. Pratesi A, Medici A, Bresci R et al (2013) Sickle cell-related bone marrow complications: the utility of diffusion-weighted magnetic resonance imaging. J Pediatr Hematol Oncol 35: 329–330
53. Littooij AS, Kwee TC, Enriquez G et al (2017) Whole-body MRI reveals high incidence of osteonecrosis in children treated for Hodgkin lymphoma. Br J Haematol 176:637–642

54. Darge K, Jaramillo D, Siegel MJ (2008) Whole-body MRI in children: current status and future applications. Eur J Radiol 68:289–298
55. Orsso CE, Mackenzie M, Alberga AS et al (2017) The use of magnetic resonance imaging to characterize abnormal body composition phenotypes in youth with Prader-Willi syndrome. Metabolism 69:67–75
56. Norman W, Jawad N, Jones R et al (2016) Perinatal and paediatric post-mortem magnetic resonance imaging (PMMR): sequences and technique. Br J Radiol 89:20151028
57. Shruthi M, Gupta J, Jana M et al (2018) Conventional vs. virtual autopsy with postmortem MRI in phenotypic characterization of stillbirths and malformed fetuses. Ultrasound Obstet Gynecol 51: 236-245